MT25
25th International Conference on Magnet Technology
RAI - Amsterdam
August 27 - September 1, 2017

Center for Advanced Electrical Machines & Drives
Huazhong University of Science and Technology

Design and Analysis of a Novel Large Mover Slot Opening Flux-Reversal Linear Permanent Magnet Machine with HTS Bulks

Chaojie Shi[1], Ronghai Qu[1], Baoquan Kou[2], Dawei Li[1], and Yuting Gao[1]

[1]State Key Laboratory of Advanced Electromagnetic Engineering, School of Electrical and Electronic Engineering, Huazhong University of Science and Technology, Wuhan 430074, China.
[2]Department of Electrical Engineering, Harbin Institute of Technology, Harbin 150001, China.

Outline

- **Background**
- **Configurations**
- **Operation Principle**
- **Performance Comparison**
- **Conclusion**

Outline

- Background
- Configurations
- Operation Principle
- Performance Comparison
- Conclusion

➢ Background

Conventional Rotary-to-linear Motion System

Linear Machine

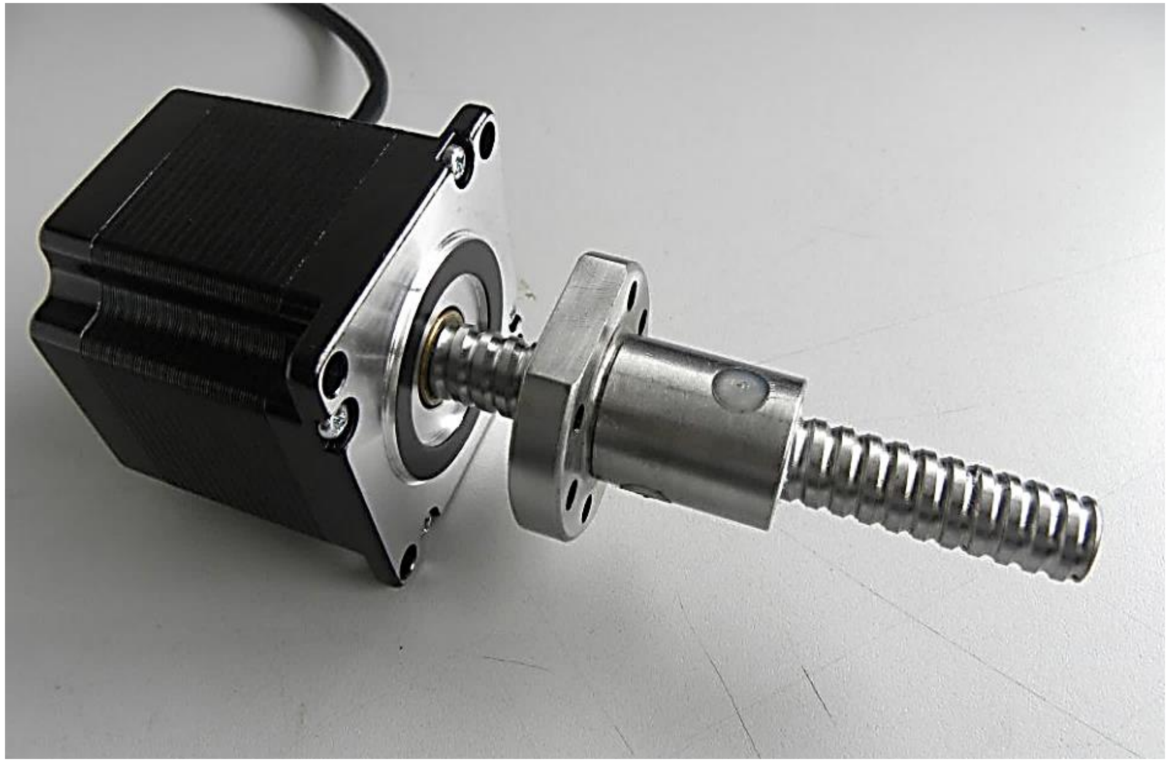

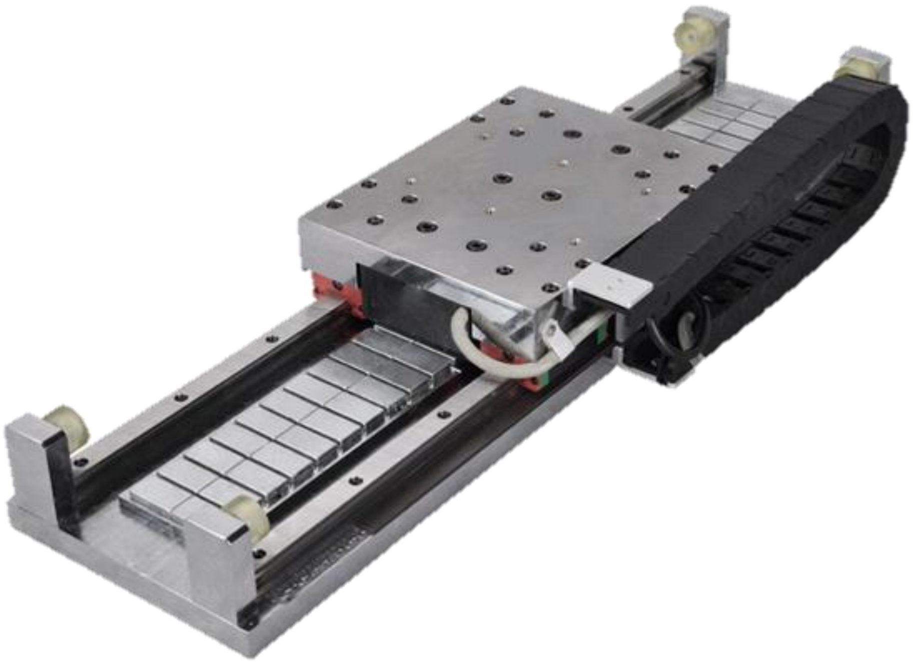

Rotary Machine + Ball screw

Direct Drive

Low efficiency
Low stability
Slow dynamic response
…

High efficiency
High stability
Fast dynamic response
…

➢ Background

Advantages of the linear machine compared to the conventional rotary-to-linear motion system:

- High efficiency
- Simple structure
- Easy maintenance
- Good heat-dissipating condition
- Fast dynamic response
- Low noise level
- …

Advantages of the flux-reversal permanent magnet machine:

- High efficiency
- Simple structure
- Robust rotor
- High torque density
- Produce large torque at low speed
- …

Flux-Reversal Linear Permanent Magnet Machine

➢ Background

Existing Flux-Reversal Linear Permanent Magnet Machine:

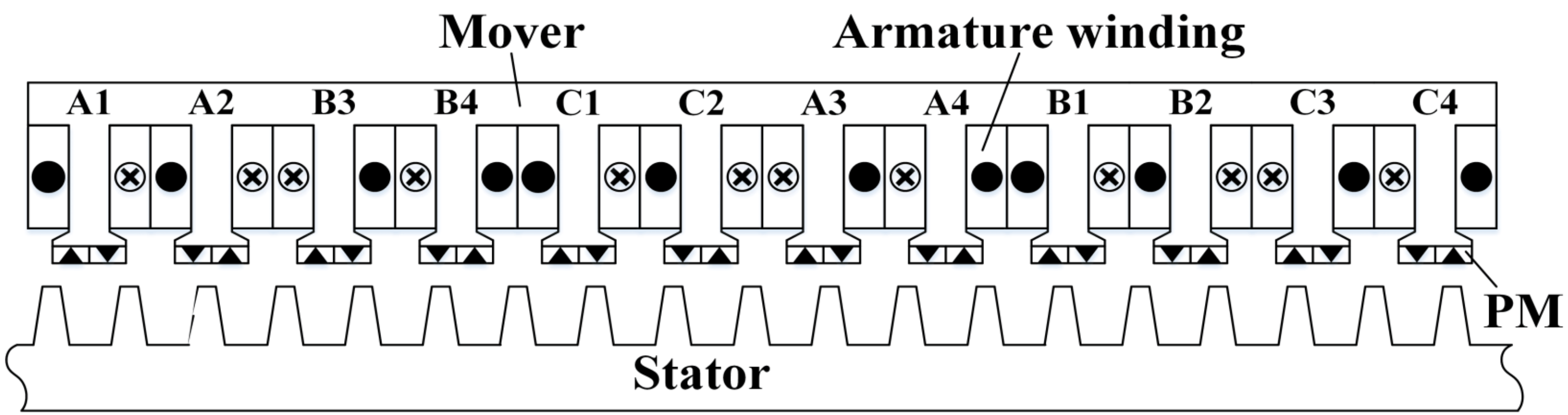

How to further improve the machine **thrust density**?

- ➢ Enhance the magnetic field. ➡ Use more PMs, but the iron core is easy to be **saturated**.
- ➢ Improve the electrical loading, i.e. improve the current. ➡ **More mover slot area** is needed. √
- ➢ Improve the flux modulation effect of the stator teeth. ➡ Adopting the **HTS bulks** and thus the **flux leakage** can be reduced. √

Outline

- Background
- **Configurations**
- Operation Principle
- Performance Comparison
- Conclusion

➢ Configurations

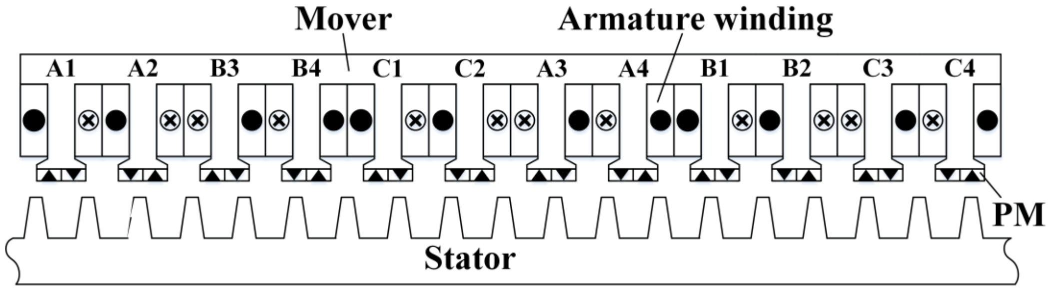

Regular Flux Reversal Linear PM Machine (FRLPM)

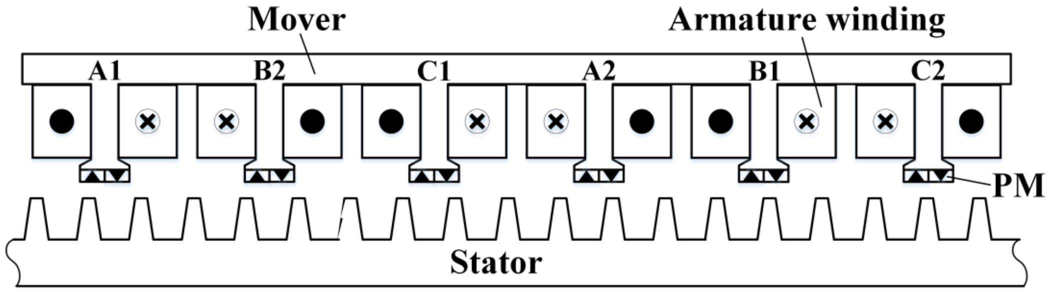

Proposed Large Mover Slot Opening FRLPM (LSO-FRLPM)

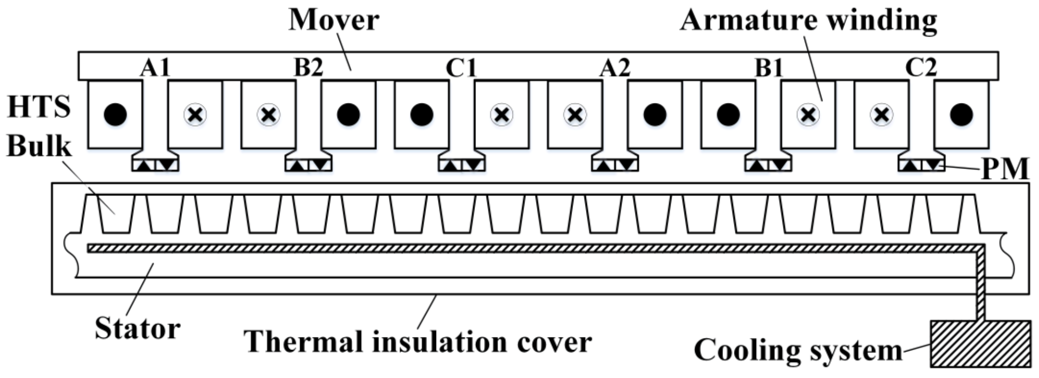

Proposed HTS LSO-FRLPM

- By **removing half of the teeth** of the regular FRLPM, the proposed LSO-FRLPM can be obtained.
- The **HTS bulks** are inserted in the **stator slots** of the LSO-FRLPM, which is the proposed HTS LSO-FRLPM.
- The regular FRLPM and LSO-FRLPM **share the same stator** configuration.
- The HTS LSO-FRLPM has **larger air-gap length** due to the adoption of the **thermal insulation cover**.

➢ Configurations

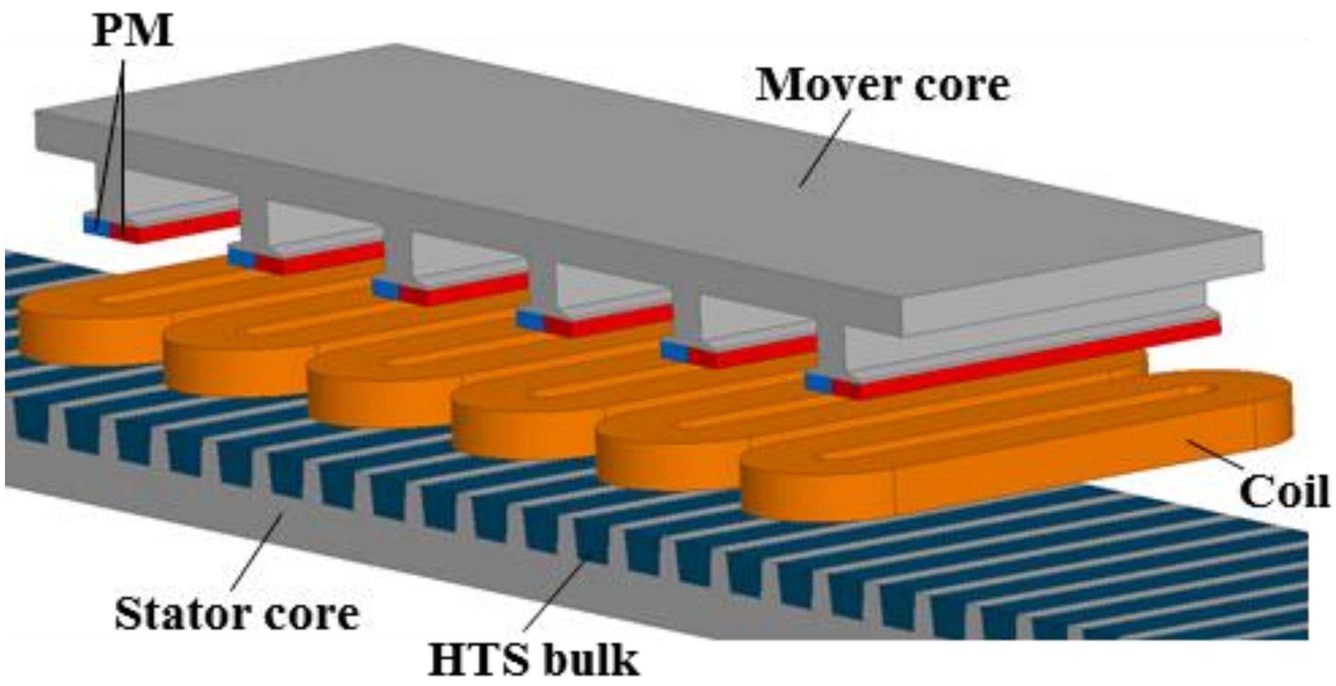

3-D Sketch of the Proposed LSO-FRLPM (Effective Part)

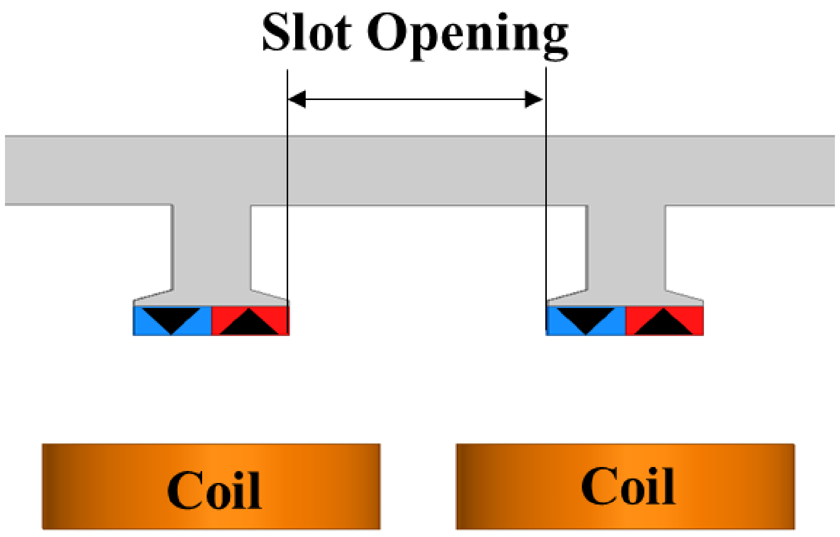

Partial View of the Mover Slot

- The concentrated windings are adopted in the HTS LSO-FRLPM.
- The PMs mounted on the adjacent mover tooth have the same arrangement, while the PM arrangement of the adjacent mover teeth is opposite in the regular FRLPM.
- The mover slot opening is much larger than the regular FRLPM due to the removing of half of the mover teeth.

Outline

- ➢ Background
- ➢ Configurations
- ➢ **Operation Principle**
- ➢ Performance Comparison
- ➢ Conclusion

➢ Operation Principles

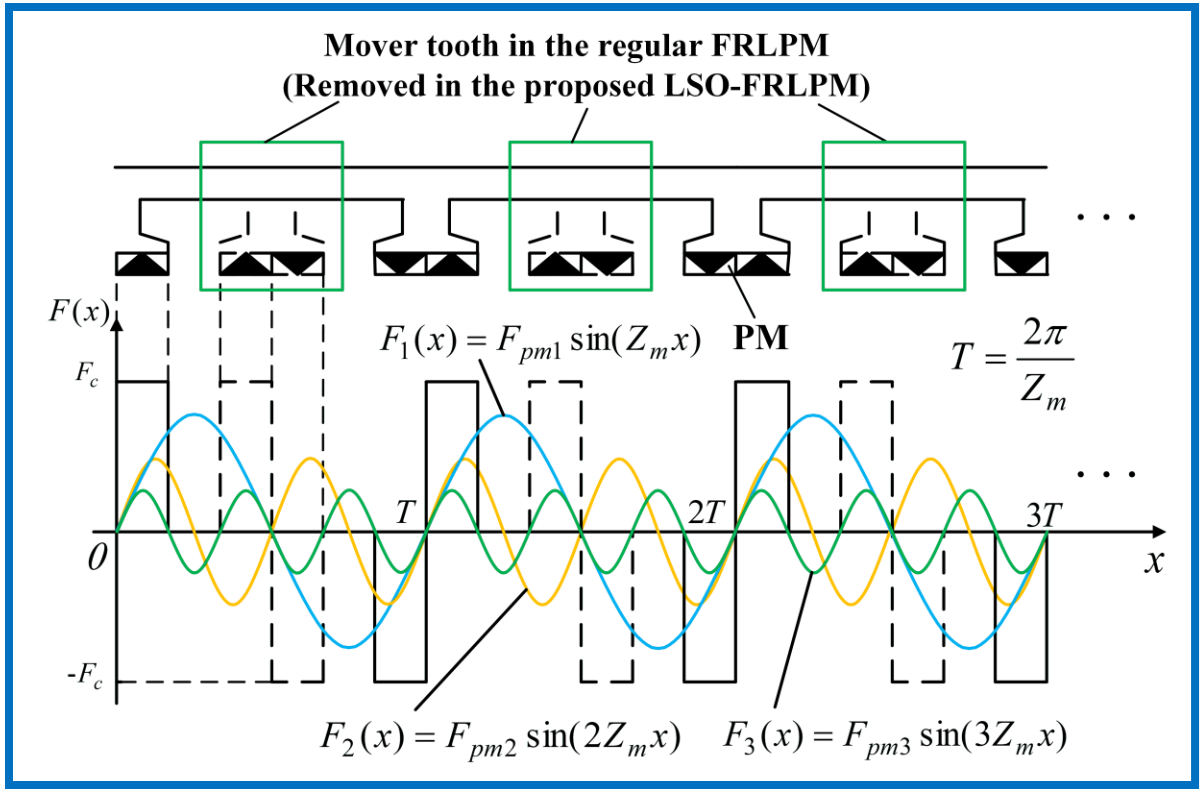

$$F_{pm}(x,t) = \sum_{i=1,2,3\ldots}^{\infty} F_{pmi}\sin[iZ_m(x - vt)]$$

- The Fourier Series of the Magnetic Motive Force (MMF) contains both odd and even harmonics, while only odd harmonics exist in the MMF of the regular FRLPM.

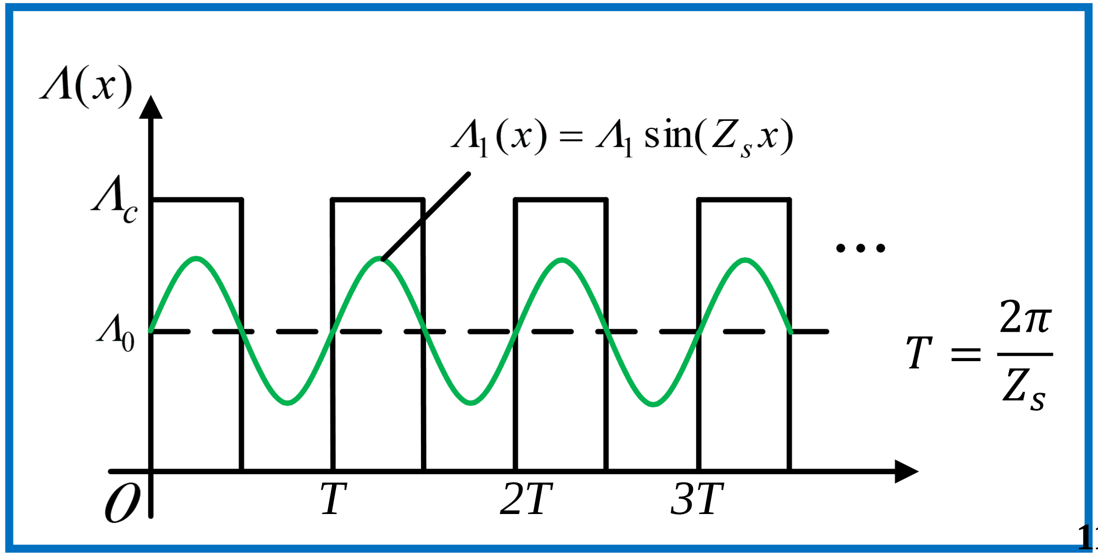

- The air-gap permeance function can be expressed as:

$$\Lambda(x) \approx \Lambda_0 + \Lambda_1\sin(Z_s x)$$

➢ Operation Principles

$$F_{pm}(x,t) = \sum_{i=1,2,3...}^{\infty} F_{pmi} \sin[iZ_m(x-vt)]$$

$$\Lambda(x) \approx \Lambda_0 + \Lambda_1 \sin(Z_s x)$$

$$B_g(x,t) = F_{pm}(x,t) \bullet \Lambda(x)$$

$$= \sum_{i=1,2,3...}^{\infty} \Lambda_0 F_{pmi} \sin[iZ_m(x-vt)]$$

$$+ \sum_{i=1,2,3...}^{\infty} \frac{1}{2}\Lambda_1 F_{pmi} \begin{Bmatrix} \cos[(iZ_m - Z_s)x + iZ_m vt] \\ -\cos[(iZ_m + Z_s)x - iZ_m vt] \end{Bmatrix}$$

➢ **Pole-pair number of the air-gap magnetic field.**

$$\lambda_{ph}(t) = L_{ef}\int_0^{2\pi} B_g(x,t) \bullet N(x,t)dx$$

$$N(x,t) = \sum_{j=1,3,5...}^{\infty} \frac{2N_w}{j\pi P_a} K_{wj} \cos[jP_a(x-vt)]$$

$$E_{ph}(t) = -\frac{d\lambda_{ph}(t)}{dt}$$

$$= \sum_{\substack{i=1,2,3... \\ m=(iZ_m+Z_s)/P_a \in N_{>0} \\ n=(iZ_m-Z_s)/P_a \in N_{>0}}}^{\infty} \left[v\frac{Z_s}{P_a} L_{ef} N_w F_{pmi} \Lambda_1 \bullet \left(\frac{K_{wm}}{m} - \frac{K_{wn}}{n} \right) \cos(Z_s vt) \right]$$

➢ **Pole-pair number of the back-EMF.**

➢ Operation Principles

Important massages from the equations:

- **All MMF harmonics (F_1, F_2, F_3…) contribute to the back-EMF and the frequency of the back-EMF is determined by the stator slots number Z_s.**

- **The armature windings pole-pair P_a is chose to be as small as possible in order to have a larger back-EMF, and thus the relationship between the mover teeth number Z_m, the stator teeth number Z_s, and the armature winding pole-pair P_a can be obtained as:**

$$P_a = \min\left\{ \begin{array}{l} P_a = |iZ_m \pm Z_s|; \dfrac{Z_m}{GCD(Z_m, P_a)} = 3k \\ i = 1,2,3\ldots; \quad k = 1,2,3\ldots \end{array} \right\}$$

➢ Operation Principles

➢ **The flux distribution variation with different mover position of the proposed LSO-FRLPM:**

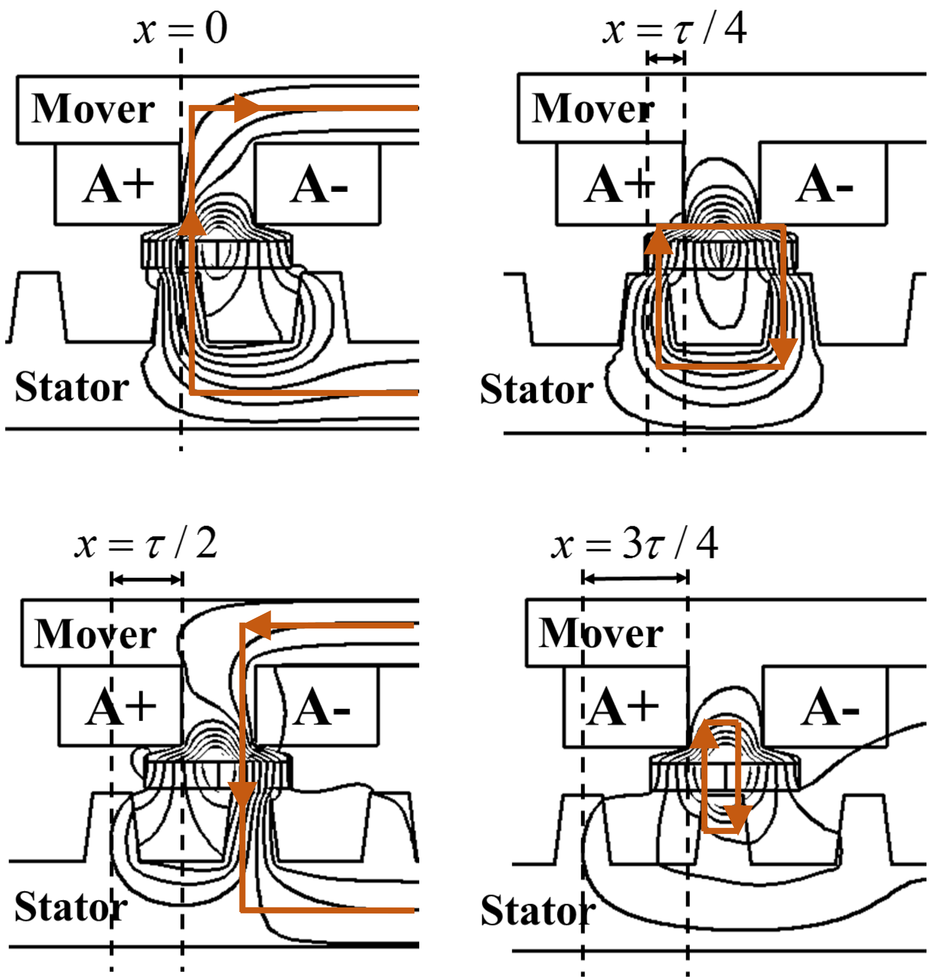

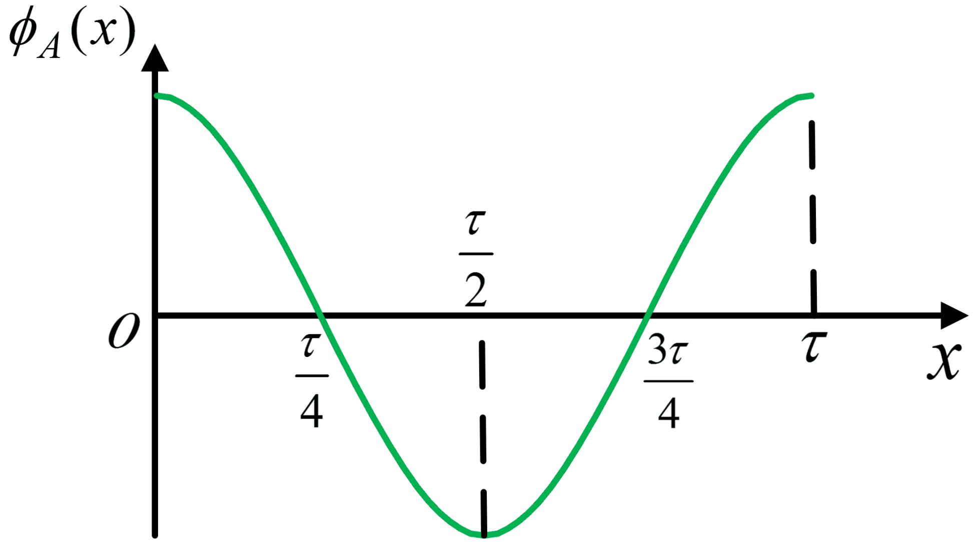

- **The flux linkage of phase A reach its positive and negative peak value at the mover position $x = 0$ and $x = \tau/2$.**
- **In the mover position $x = \tau/4$ and $x = 3\tau/4$, the flux linkage of phase A equals zero.**
- **The main flux linkage of phase A is depicted in the figures.**

Outline

- Background
- Configurations
- Operation Principle
- **Performance Comparison**
- Conclusion

➢ Performance Comparison

➢ **Three FEM models about the regular FRLPM, LSO-FRLPM and HTS LSO-FRLPM are built to compared with each other:**

Regular FRLPM

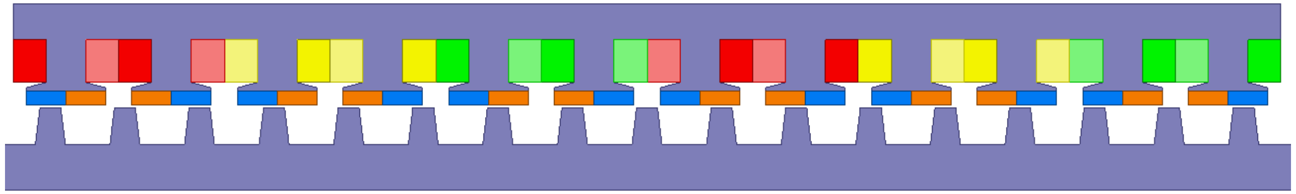

LSO-FRLPM

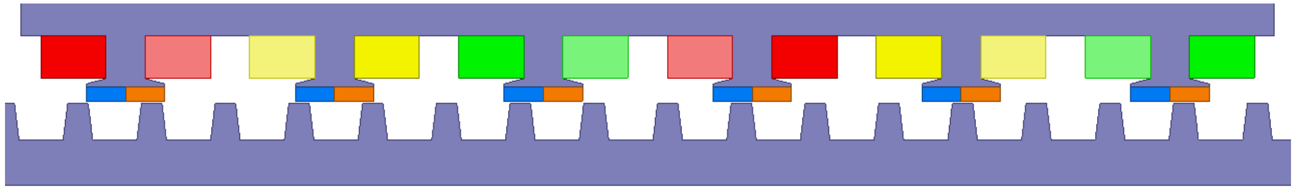

HTS LSO-FRLPM

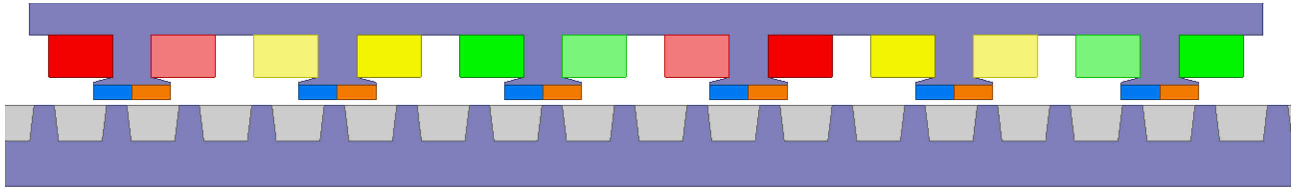

Geometry Parameters of the Models

Machine	Regular FRLPM	LSO-FRLPM	HTS LSO-FRLPM
Mover width, L (mm)	312		
Mover height, h_{mover} (mm)	25		
Mover tooth number, Z_m	12	6	6
Mover slot opening ratio	0.25	0.625↑	0.625↑
Mover slot area, A_{slot} (mm^2)	2311	3136↑	3136↑
Cost of PMs (kg)	0.63	0.32↓	0.32↓
Air-gap length, g (mm)	0.6	0.6	1.5↑
Thickness of PMs, h_m (mm)	3.6		
Stack length, L_{ef} (mm)	100		
Stator tooth number, Z_s	17		

➢ Performance Comparison

➢ **The three FRLPMs are compared with each other in terms of flux linkage, back-EMF and average thrust:**

Flux linkage

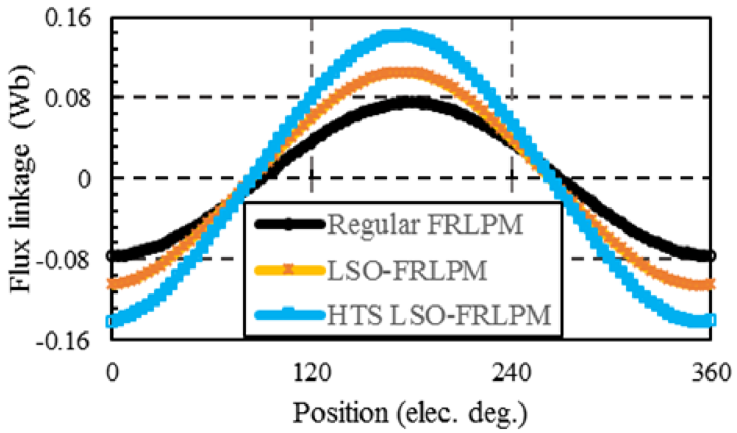

Back-EMF

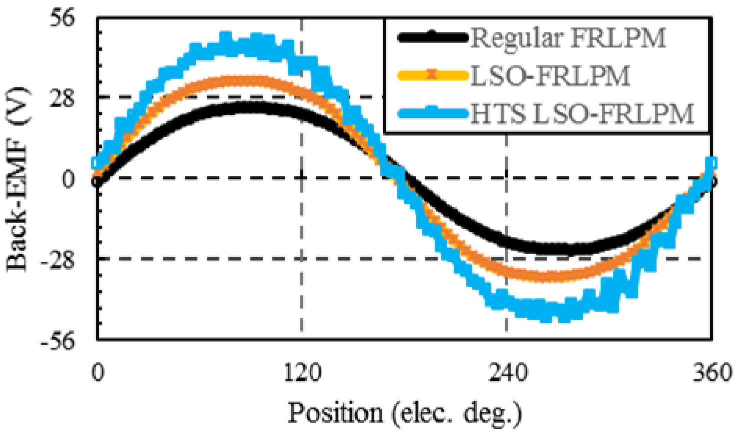

Average Thrust

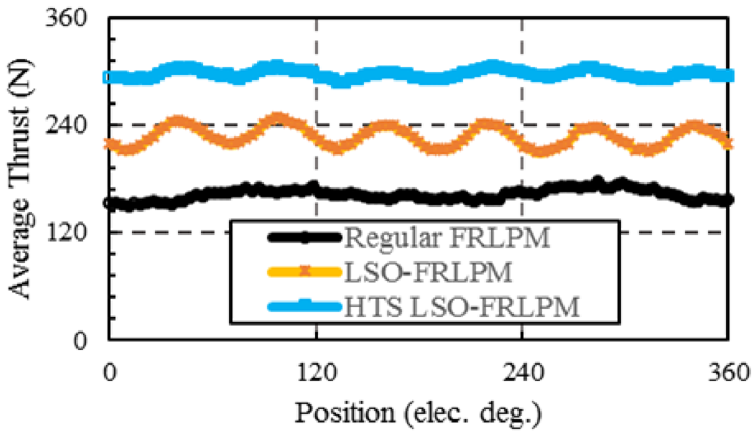

Performance Comparison

Machine	Regular FRLPM	LSO-FRLPM	HTS LSO-FRLPM
Rated phase current, I (RMS, A)		3	
Current density, J (A/mm^2)		6.4	
Turns of coils per phase	296	401	401
Winding factor	0.25	0.5↑	0.5↑
Flux-linkage per phase, Ψ (RMS, Wb)	0.053	0.074↑	0.099↑
Back-EMF (RMS, V)	18.2	25.3↑	34.1↑
Average thrust (N)	162.4	227.3↑	296.7↑
Thrust ripple (%)	8.1	8.7↑	3.0↓

- **Flux-linkage, back-EMF and average thrust of both LSO-FRLPM and HTS LSO-FRLPM are significantly improved compared to the regular FRLPM.**
- **HTS LSO-FRLPM shows the best performance.**

Outline

- Background
- Configurations
- Operation Principle
- Performance Comparison
- **Conclusion**

➢ Conclusion

- A novel large mover slot opening FRLPM (LSO-FRLPM) class is proposed in this paper.
- The air-gap flux density, back-EMF of the LSO-FRLPM are analytical derived in the paper and thus the operation principle of the proposed machine can be explained clearly.
- The proposed LSO-FRLPM with or without HTS bulks are compared with the regular FRLPM using the finite element method (FEM). The superiority of the LSO-FRLPM is verified by the FEM results.
- The LSO-FRLPM can produce a 40% higher average thrust than that of the regular FRLPM when the PM consumption of the LSO-FRLPM is only half of that of the regular FRLPM.
- The average thrust of the HTS LSO-FRLPM is 83% and 30% higher than that of the regular FRLPM and the LSO-FRLPM, and the thrust ripple of the HTS LSO-FRLPM is reduced by 63% and 66% compared to the regular FRLPM and the LSO-FRLPM.

Thanks for listening!

E-mail: chaojieshi@hust.edu.cn